

## NON-LINEAR FRACTURE BEHAVIOR OF DOUBLE CANTILEVER BEAM

Viktor Rizov\*

*This article describes a theoretical study of non-linear fracture behavior of the Double Cantilever Beam (DCB) configuration. The fracture is analyzed using the  $J$ -integral approach. A stress-strain curve with power-law hardening is used for describing the mechanical response of the DCB. It is assumed that the material has the same properties in tension and compression. A model based on Mechanics of materials is applied to find solutions of the  $J$ -integral at different levels of the external load. The effect of the exponent of the power law on the non-linear fracture behavior is evaluated. It is found that if higher values of the exponent of the power law are used, the  $J$ -integral value increases. The analytical approach developed here is very useful for parametric investigations, since it captures by relatively simple formulae the essential of the non-linear fracture.*

Keywords non-linear fracture analysis, beam theory,  $J$ -integral, hardening

### 1. Introduction

With the increasing use of laminates in load-bearing structures, an extensive knowledge of their fracture behavior is highly required. Crack propagation is one of the main life-limiting failure modes in laminates. Crack considerably reduce stiffness and may lead to catastrophic failure of the laminate structure. Much effort has been devoted to study the fracture properties of laminates under static loading conditions [1–14]. For this purpose, various beam configurations have been developed. Mode I delamination fracture behavior has been investigated mainly by the DCB specimen [1, 2]. In these investigations, fracture usually is studied using linear-elastic fracture mechanics which is based on the assumptions for validity of the Hook's law. However, in laminated systems of high fracture toughness, plastic strains can develop prior to the onset of crack growth. Thus, the material non-linearity should be taken into account in fracture analyses.

The purpose of the present paper is to perform a theoretical study of non-linear fracture in the DCB configuration. Fracture is analyzed using the  $J$ -integral approach in conjunction with a model based on Mechanics of materials. A stress-strain curve with power-law hardening is applied. The influence of the power law exponent on the fracture is evaluated.

### 2. $J$ -integral analysis

The geometry of the DCB configuration analyzed in the present article is reported in Fig. 1. The external loading consists of two moments,  $M$ , applied at the end of the crack arms. There is an initial crack of length  $a$  in the mid-plane of the beam.

---

\* Prof. Dr. V. Rizov, Department of Technical Mechanics, University of Architecture, Civil Engineering and Geodesy, 1 Chr. Smirnensky Blvd., 1046 – Sofia, Bulgaria

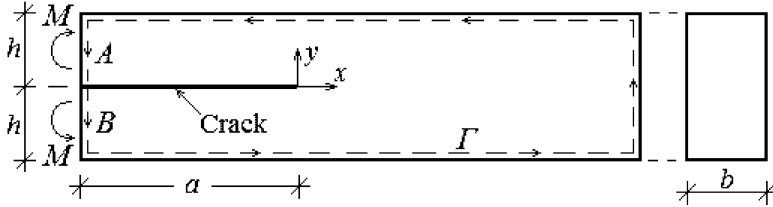


Fig.1: Geometry and loading of the DCB

It is assumed that the mechanical behavior of the DCB follows the non-linear stress-strain curve shown in Fig. 2. The curve has two sections. The initial linear section, OC, is followed by a non-linear section, CD, with power-law hardening (Fig. 2). The stress-strain relation in the non-linear section is written as

$$\sigma = f_y \left( \frac{\varepsilon}{\varepsilon_y} \right)^m, \quad (1)$$

where  $f_y$  is the yield stress limit of the material,  $\varepsilon_y$  is the strain that corresponds to  $f_y$ , and  $m$  is the exponent of the power-law.

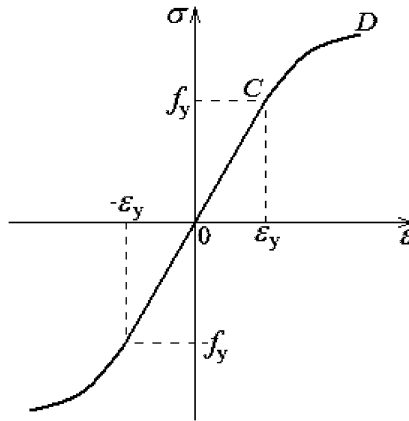


Fig.2: Stress-strain curve with power-law hardening

The non-linear fracture behavior of the DCB specimen is analyzed by applying the integration contour independent  $J$ -integral [15, 16]. Therefore, the integration contour is chosen to coincide with the beam contour as illustrated in Fig. 1. In this way, the  $J$ -integral solution is substantially facilitated. It is obvious that the  $J$ -integral value is non-zero only in segments A and B of the contour (Fig. 1). Due to the symmetry conditions, it is enough to solve the  $J$ -integral in segment A and to double the result obtained. The  $J$ -integral is written as [17]

$$J = \int_{\Gamma} \left[ u_0 \cos \alpha - \left( p_x \frac{\partial u}{\partial x} + p_y \frac{\partial v}{\partial x} \right) \right] ds, \quad (2)$$

where  $\Gamma$  is a contour of integration going around the crack from one crack face to the other in the counter clockwise direction,  $u_0$  is the strain energy density,  $\alpha$  is the angle between the outwards normal vector to the contour of integration and the crack direction,  $p_x$  and  $p_y$  are the components of the stress vector,  $u$  and  $v$  are the components of the displacement

vector with respect to the crack tip coordinate system,  $xy$ , and  $ds$  is a differential element along the contour  $\Gamma$ .

At low magnitudes of the external loading, the DCB configuration will deform in linear-elastic stage (the Hook's law is valid). In this case, the normal stress,  $p_x$ , in segment A is obtained using the equation :

$$p_x = \frac{M}{I} y_1 , \tag{3}$$

where  $I = bh^3/12$  is the principal moment of inertia of the upper crack arm cross-section (here  $b$  is the width of beam cross-section). The vertical coordinate,  $y_1$ , varies in the interval  $[-h/2, h/2]$ , and  $ds = -dy_1$ ,  $\cos \alpha = -1$ ,  $p_x = 0$ .

The following formula from Mechanics of materials is used to obtain the partial derivative

$$\frac{\partial u}{\partial x} = -\varepsilon_x = -\frac{p_x}{E} = -\frac{M}{EI} y_1 . \tag{4}$$

where  $E$  is the modulus of elasticity.

The strain energy density is obtained as

$$u_0 = \frac{p_x^2}{2E} = \frac{1}{2E} \left[ \frac{M}{I} y_1 \right]^2 = \frac{M^2}{2EI^2} y_1^2 . \tag{5}$$

We substitute (3), (4) and (5) in (2). Thus, the linear-elastic  $J$ -integral solution is

$$J = 2 \int_{-\frac{h}{2}}^{\frac{h}{2}} \left[ \frac{M^2}{2EI^2} y_1^2 (-1) - \frac{M}{I} y_1 \left( -\frac{M}{EI} y_1 \right) \right] (-dy_1) = \frac{12 M^2}{E b^2 h^3} . \tag{6}$$

It is known that at linear-elastic behaviour, the  $J$ -integral value coincides with the strain energy release rate. This fact is used here to verify the solution (6). Indeed, (6) coincides with the expression for the strain energy release rate in the DCB configuration reported in [18].

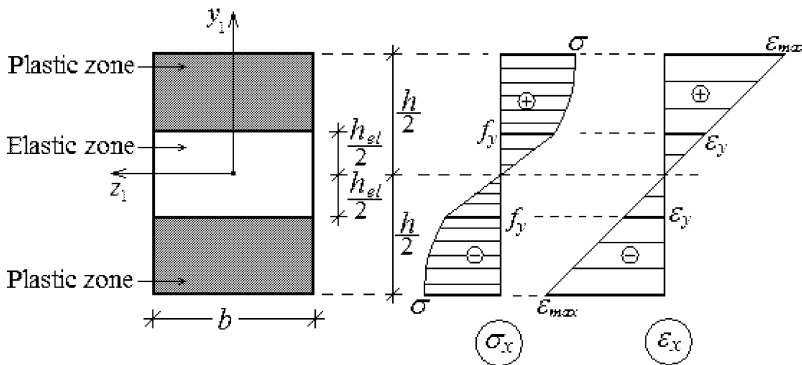


Fig.3: Distribution of normal stresses and linear strains in the crack arms

If the fracture toughness is high, plastic strains will arise prior to the onset of crack growth from the initial crack tip position. Two symmetric plastic zones will be developed in the crack arms as illustrated in Fig. 3. The value of the  $J$ -integral in segment A is obtained by integration along the elastic and plastic zones, i.e.

$$J = J_{el} + J_{pl} , \quad (7)$$

where the  $J$ -integral in the elastic zone of the crack arm cross-section is written as

$$J_{el} = \int_{\frac{h_{el}}{2}}^{-\frac{h_{el}}{2}} \left[ u_0 \cos \alpha - \left( p_x \frac{\partial u}{\partial x} \right) \right] ds , \quad (8)$$

where  $h_{el}$  is the height of the elastic zone (Fig. 3).

The normal stresses in the elastic zone are distributed linearly (refer to formula (3)).

The partial derivative,  $\partial u / \partial x$ , is written as:

$$\frac{\partial u}{\partial x} = -\varepsilon_x = -\frac{1}{\rho} y_1 , \quad (9)$$

where  $1/\rho$  is the curvature of the crack arm in elastic-plastic stage of deformation.

We will use the equation for equilibrium of the elementary forces in the cross-section of the crack arm in order to determine  $1/\rho$  (Fig. 3). The equation is written as

$$M = \frac{b h^2}{2 \varepsilon_{\max}^2} \int_0^{\varepsilon_{\max}} \sigma(\varepsilon) \varepsilon d\varepsilon , \quad (10)$$

or

$$M = \frac{b h^2}{2 \varepsilon_{\max}^2} \left( \int_0^{\varepsilon_y} E \varepsilon \varepsilon d\varepsilon + \int_{\varepsilon_y}^{\varepsilon_{\max}} f_y \frac{\varepsilon^m}{\varepsilon_y^m} \varepsilon d\varepsilon \right) . \quad (11)$$

After transformations and taking into account the fact that

$$\varepsilon_{\max} = \frac{h}{2} \frac{1}{\rho} , \quad (12)$$

equation (11) is written as

$$\kappa^{2+m} + c \kappa^2 + d = 0 , \quad (13)$$

where

$$\kappa = \frac{1}{\rho} , \quad (14)$$

$$c = -\frac{2^{m+1} (m+2) M f_y^{m-1}}{b h^{2+m} E^{2+m}} , \quad (15)$$

$$d = \frac{4 (m-2) 2^m f_y^{2+m}}{3 h^{2+m} E^{2+m}} . \quad (16)$$

Obviously, at  $m = 0$  the power law (1) transforms into the constitutive law of the elastic-perfectly plastic material, i.e.  $\sigma = f_y$ . This fact is used here to verify (13). For this purpose, we substitute  $m = 0$  in (15) and (16) and then solve equation (13) with respect to  $\kappa$ . The result is

$$\frac{1}{\varrho} = \frac{1}{\varrho_s} \frac{1}{\sqrt{3 - 2 \frac{M}{M_y^{(s)}}}}, \quad (17)$$

where

$$\frac{1}{\varrho_s} = \frac{2 f_y}{h E}, \quad (18)$$

$$M_y^{(s)} = \frac{b h^2}{6} f_y. \quad (19)$$

Here  $M_y^{(s)}$  is the moment at which the normal stress in the remotest edges of the crack arm cross-section attains the material yield stress limit. Equation (17) coincides with the formula for the curvature, when the elastic-perfectly plastic model is used [19], which verifies (13). Another verification of (13) is performed by using the fact that at  $m = 1$  equation (1) transforms into the Hook's law. Indeed, after substitution of  $m = 1$  in (15) and (16), from (13) we obtain

$$\frac{1}{\varrho} = \frac{M}{E I}, \quad (20)$$

which is the curvature when the linear-elastic model is used.

The strain energy density is found as

$$u_0 = \frac{1}{2} p_x \varepsilon_x = \frac{M}{2 I} \frac{1}{\varrho} y_1^2, \quad (21)$$

where the curvature,  $1/\varrho$ , is obtained by equation (13).

By substitution of (3), (9), and (21) in (8), we obtain

$$J_{el} = \frac{M}{2 b h^3} \frac{1}{\varrho} h_{el}^3, \quad (22)$$

The height of the elastic zone (Fig. 3) is determined using the following formula from Mechanics of materials [19]:

$$h_{el} = \frac{2 f_y}{E \frac{1}{\varrho}}. \quad (23)$$

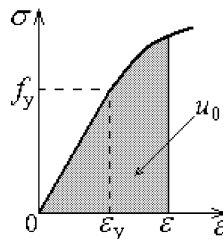


Fig.4: Determination of the strain energy density in the plastic zones of the crack arms

The  $J$ -integral in the plastic zones of the crack arm cross-section is written as

$$J_{\text{pl}} = 2 \int_{\frac{h_{\text{el}}}{2}}^{\frac{h}{2}} \left[ u_0 \cos \alpha - \left( p_x \frac{\partial u}{\partial x} \right) \right] ds, \quad (24)$$

where the Figure 2 takes into account the fact that there are two symmetric plastic zones in the crack arm cross-section (Fig. 3).

The normal stresses in the plastic zones are obtained by formula (1). Equation (9) is used to obtain the partial derivative. The strain energy density in the plastic zones of the crack arm cross-section is equal to the area enclosed by the stress-strain curve [20, 21, 22, 23], i.e.

$$u_0 = \frac{1}{2} f_y \varepsilon_y + \int_{\varepsilon_y}^{\varepsilon} f_y \left( \frac{\varepsilon}{\varepsilon_y} \right)^m d\varepsilon. \quad (25)$$

By substitution of  $\varepsilon = (1/\rho) y_1$  and  $\varepsilon_y = f_y/E$  in (25) and solving the integral, we obtain

$$u_0 = \frac{f_y^2}{2E} + \frac{E^m}{m+1} f_y^{1-m} \left( \frac{1}{\rho} \right)^{m+1} y_1^{m+1} - \frac{f_y^2}{E(m+1)}. \quad (26)$$

We substitute (1), (9) and (26) into (24). The solution of (24) is

$$J_{\text{pl}} = \frac{f_y^2}{E} \frac{1-m}{m+1} \left( \frac{h}{2} - \frac{h_{\text{el}}}{2} \right) + \frac{m}{(m+1)(m+2)2^{m+1}} E^m f_y^{1-m} \left( \frac{1}{\rho} \right)^{m+1} (h^{m+2} - h_{\text{el}}^{m+2}). \quad (27)$$

where  $h_{\text{el}}$  is obtained by (23).

By substitution of (22) and (27) into (7), we obtain the  $J$ -integral solution in segment A (Fig. 1)

$$J = \frac{M}{2bh^3} \frac{1}{\rho} h_{\text{el}}^3 + \frac{f_y^2}{E} \frac{1-m}{m+1} \left( \frac{h}{2} - \frac{h_{\text{el}}}{2} \right) + \frac{m}{(m+1)(m+2)2^{m+1}} E^m f_y^{1-m} \left( \frac{1}{\rho} \right)^{m+1} (h^{m+2} - h_{\text{el}}^{m+2}). \quad (28)$$

The final solution is obtained by doubling (28) in view of the symmetry, i.e.

$$J = \frac{M}{bh^3} \frac{1}{\rho} h_{\text{el}}^3 + \frac{f_y^2}{E} \frac{1-m}{m+1} (h - h_{\text{el}}) + \frac{m}{(m+1)(m+2)2^m} E^m f_y^{1-m} \left( \frac{1}{\rho} \right)^{m+1} (h^{m+2} - h_{\text{el}}^{m+2}). \quad (29)$$

In formulae (26)–(29), the curvature,  $1/\rho$ , is obtained by equation (13).

It should be mentioned that at  $m = 1$ , equation (29) transforms into the linear-elastic solution (6).

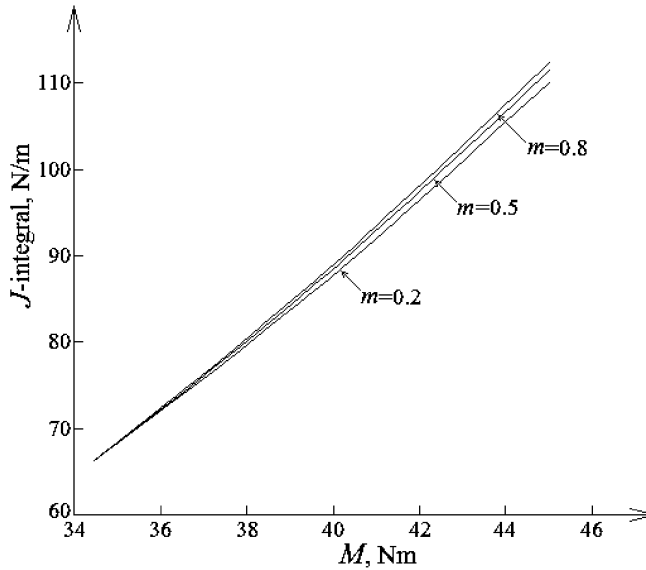


Fig.5: The  $J$ -integral value plotted against the external moment,  $M$ , at three magnitudes of the power-law exponent,  $m$

The influence of the exponent,  $m$ , on the non-linear fracture in the DCB configuration is evaluated. For this purpose, the  $J$ -integral value is calculated by (29) at different magnitudes of  $m$ . The following dimensions of the crack arm cross-section are used:  $b = 0.02$  m and  $h = 0.01$  m. Calculations are performed for magnitudes of the external moment,  $M$ , higher than  $M_y^{(s)}$  (refer to formula (19)). Thus, the beam deforms in elastic-plastic stage. It is assumed also that  $E = 5.378 \times 10^{11}$  Pa and  $f_y = 1.034 \times 10^8$  Pa. In these calculations, the curvature,  $1/\rho$ , is determined by equation (13) using the Matlab program system. The results of the  $J$ -integral calculations are presented graphically in Fig. 5. The diagrams in Fig. 5 indicate that the  $J$ -integral value increases when  $m$  increases. Certainly, at the elastic limit load of  $M = M_y^{(s)} = 34.47$  Nm the power law exponent,  $m$ , does not influence the  $J$ -integral value, since in this case the plastic zone size is zero.

### 3. Conclusions

A theoretical investigation of non-linear fracture behavior of the DCB configuration is performed. For this purpose, a stress-strain curve with power-law hardening is used. The fracture is analyzed by the integration contour independent  $J$ -integral. A model based on Mechanics of materials is applied to find the  $J$ -integral solutions. An equation is derived of the crack arm curvature in elastic-plastic stage of deformation. The influence of the material hardening on the fracture behavior is investigated. For this purpose, calculations of the  $J$ -integral value at different magnitudes of the exponent,  $m$ , are performed. It is found that the  $J$ -integral value increases when  $m$  increases. The non-linear solutions obtained in the present article can be applied for calculation of the critical  $J$ -integral value by using experimentally determined critical load at the onset of crack growth from the initial crack tip position in the DCB specimen. The analytical approach used here is very suitable for performing parametrical investigations, since the simple formulae obtained capture the essential of the non-linear fracture behavior.

## References

- [1] Robinson P.M., Song D.Q.: A modified DCB specimen for Mode I testing of multidirectional laminates, *J. Compos. Mater.* 16 (1992), 1554–1577
- [2] Brunner A.J.: Experimental aspects of Mode I and Mode II fracture toughness testing of fiber-reinforced polymer-matrix composites, *Comput. Methods Appl. Mech. Eng.* 185 (2000), 161–172
- [3] Suemasu H.: Double Notched Split Cantilever Test Method to Measure the Mixed Mode II and III Interlaminar Toughness, *Proceedings 17th International Conference on Composite Materials*, Edinburgh, UK, 2009, 175–183
- [4] De Moraes A., Pereira A.: Mixed Mode II+III Interlaminar Fracture of Carbon/Epoxy Laminates, *Composites Science and Technology* 68 (2008), 2022–2027
- [5] Szekrényes A.: Interlaminar Fracture Analysis in the  $G_I$ - $G_{II}$ - $G_{III}$  Space Using Prestressed Transparent Composite Beams, *Journal of Reinforced Plastics and Composites* 30 (2011), 1655–1669
- [6] Szekrényes A.: The influence of crack length and delamination width on the mode III energy release rate of laminated composites, *Journal of Composite Materials* 45 (2011), 279–294
- [7] Szekrényes A.: Interlaminar stresses and energy release rates in delaminated orthotropic composite plates, *International Journal of Solids and Structures* 49 (2012), 2460–2470.
- [8] Blackman B.R.K., Kinloch A.J.: Fracture Tests for Structural Adhesive Joints, In: *Fracture Mechanics Testing Methods for Polymers, Adhesives and Composites*, Eds. Pavan A., Moore D.R., and Williams J.G., Elsevier Science Ltd., Oxford, UK, 2001
- [9] Martin R.H.: Interlaminar fracture characterization, *Key Eng. Mater.* (1996), 329–346
- [10] Stevanovic D., Jar P.-Y.B., Kalyanasundaram S., Lowe A.: On Crack-Initiation Conditions for Mode I and Mode II Delamination Testing of Composite Materials, *Compos. Sci. Technol.* 60 (2000), 1879–1887
- [11] Pagano N.J., Schoeppner G.A.: Delamination of polymer matrix composites: problems and assessment, *Comprehensive Composite Materials 2*, Kelly A., Zweben C. (Eds.), Elsevier Science, Oxford, 2000, 433–528
- [12] Bolotin V.V.: Delaminations in composite structures: its origin, buckling, growth and stability, *Composites: Part B* 27B (1996), 129–145
- [13] Benzeggagh M.L., Kenane M.: Measurement of Mixed-mode Delamination Fracture Toughness of Unidirectional Glass/Epoxy Composites with Mixed-Mode Bending Apparatus, *Composites Science and Technology*. 56 (1996), 439–449
- [14] Kevin T.: Interlaminar Fracture Toughness: the Long and Winding Road to Standardization, *Composites Part B* 29B (1998), 57–62
- [15] Rice J.R.: A Path Independent Integral and the Approximate Analysis of Strain Concentration by Notches and Cracks, *Journal of Applied Mechanics* 35 (1968), 379–386
- [16] Cherepanov G.: *Brittle materials fracture mechanics*, 1974, Nauka, M
- [17] Broek D.: *Elementary engineering fracture mechanics*, 1986, Springer.
- [18] Hutchinson J.W., Suo Z.: Mixed Mode Cracking in Layered Materials, *Advances in Applied Mechanics* 29 (1992), 63–191
- [19] Malinin N.N.: *Applied theory of plasticity and creep*, M., 1968, Mashinostroenie
- [20] Hoff N.J.: *The analysis of structures*, John Wiley&Sons, 1956, New York
- [21] Nadai A.: *Theory of flow and fracture of solids*, Vol. 2., McGraw-Hill, 1963, New York
- [22] Seely F.B., Smith J.O.: *Advanced mechanics of materials*, John Wiley&Sons, 1967, New York
- [23] Washizu K.: *Variational methods in elasticity and plasticity*, Pergamon press, 1974, Oxford

*Received in editor's office:* February 2, 2015

*Approved for publishing:* May 30, 2015